A Novel Single-Feed Circular Microstrip Antenna With Reconfigurable Polarization Capability

Boyon Kim, *Student Member, IEEE*, Bo Pan, *Student Member, IEEE*, Symeon Nikolaou, Young-Sik Kim, *Member, IEEE*, John Papapolymerou, *Senior Member, IEEE*, and Manos M. Tentzeris, *Senior Member, IEEE*

***Abstract*—A single-feed circular microstrip antenna with reconfigurable polarization capability is proposed. This antenna has a simple structure, which consists of a radiating circular patch, five switches (PIN diode), three matching stubs, and a 50 Ω microstrip feed line. It can be switched between 4 different states: two states (low-frequency and high-frequency) for linear polarization (LP), one state for left hand circular polarization (LHCP) and one for right hand circular polarization (RHCP) by controlling the bias voltage of two PIN diodes. At the same time, three switchable matching stubs are used for matching every polarization state. Simulation results and experimental results show that the proposed antenna demonstrates a low cross polarization level, good impedance bandwidth, and a very good axial ratio in the circularly polarized states.**

***Index Terms*—Circular polarization, linear polarization, microstrip antenna, PIN diode, reconfigurable polarization.**

I. Introduction

RECONFIGURABLE microstrip antennas for frequency agility and polarization diversity have advantages of frequency reuse for doubling the system capability and a high degree of polarization control to optimize system performance [1]. Moreover, these reconfigurable antennas have been reported to achieve polarization diversity and reconfigurability [2]–[4] that offer an improved effectiveness in receiving the communication signal and have an exceptional ability of reducing multipath fading. In addition, many reconfigurable antennas with polarization diversity between linear and circular polarization [5] and two circular polarizations (i.e., LHCP and RHCP) [1]–[3] have been discussed in past literature. Due to the significant difference in the input impedance, the matching covered only one polarization state between LP and CP [5] or LHCP and RHCP [6], [7]. In [6], the impedance seems to be matched well in both LP and CP, but resonant frequencies in CP have matched in only one operation status. Although impedance matching was considered for polarizations in [8], it was not clear how input matching could be achieved by optimizing both polarization senses. Therefore, impedance matching techniques are necessary for all polarization senses. A reconfigurable matching network for the radiation pattern diversity using short and open stubs has been described in [9] for an annular slot antenna operating at 5.8 GHz. Based on the similar concept in reconfigurable matching network, the impedance matching can be obtained at both two different frequencies in LP and same frequency in LHCP or RHCP. PIN diodes which are used for switching the polarization are commonly used switching devices for RF and microwave front-end application systems, because they have attractive properties such as low insertion loss, good isolation, low power handling, and low cost [10].

In this paper, the authors present for the first time, the design, fabrication, and measurement of a novel single-feed circular microstrip antenna with reconfigurable polarization capability for all polarization states. The proposed antenna utilizes an etched "U" shaped slot line on the top of the circular microstrip patch. To switch the polarization states, two PIN diodes are installed on the inset of the "U" shaped slot line.

Full-wave simulations were carried out using IE3D with good matching performance for all polarization states [11]. Furthermore, the simulations were validated by comparing the simulated and measured results which show a good agreement between them.

Concerning the contents of this paper, Section II discusses the design process of the proposed antenna, including its geometry and operation principle for reconfigurable polarization capabilities (Section II-A), the switchable matching for all polarizations (Section II-B) and the application of PIN-diodes for the matching implementation (Section II-C). Section III focuses on the antenna performance for the both LP and CP modes. The effect of the most critical geometrical parameters on the CP performance is studied in Section IV, and finally conclusion is addressed in Section V.

II. Antenna Design With Reconfigurable Polarization Capabilities

The geometry of the proposed single-feed circular microstrip antenna is shown in Fig. 1. The circular patch of radius r_1 is etched on a sheet of RT/duroid 5880 printed circuit board (thickness, $h = 62$ mil and relative dielectric constant, $\varepsilon_r = 2.2$). For the arc slot, the inner side radius of the arc slot is r_2, and the central angle is α. The ground plane dimensions are 100×100 mm^2. The length and width of the insets are determined by the size of the PIN diode ($w_5 \times l_5$). The feed line is composed of a 50 Ω microstrip and three matching stubs (S_{O1}, S_{O2}, and S_{S3}) which are connected to the feed line by PIN diodes (#1, #2, and #3) to allow for the matching of the four different polarization states. To control the polarization

Manuscript received July 12, 2006; revised March 11, 2007.

B. Kim is with the Semiconductor Business, Samsung Electronics, Yongin 446-711, Korea (e-mail: boyonkim@gmail.com).

B. Pan, S. Nikolaou, J. Papapolymerou, and M. M. Tentzeris are with the School of Electrical and Computer Engineering, Georgia Institute of Technology, Atlanta, GA 30332 USA.

Y.-S. Kim is with the Department of Radio Sciences and Engineering, Korea University, Seoul 136-701, Korea.

Digital Object Identifier 10.1109/TAP.2008.916894

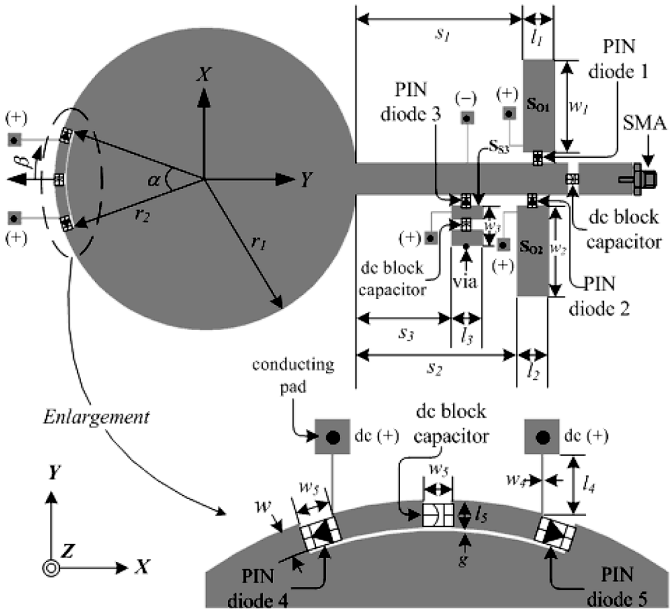

Fig. 1. Geometry of a novel single-feed circular microstrip antenna with reconfigurable polarization capabilities including the parametric study (α and β).

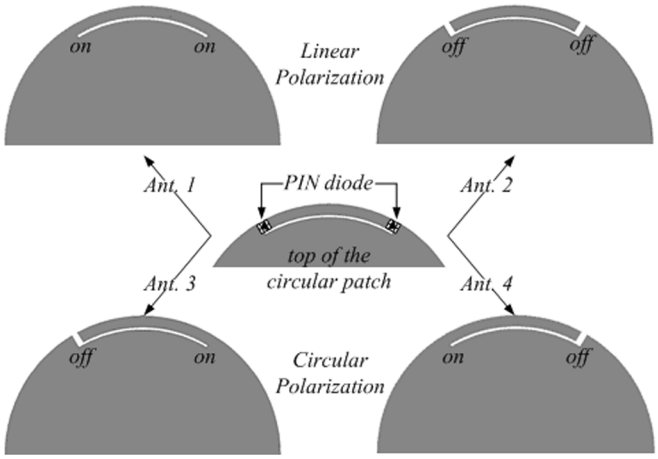

Fig. 2. The operation mechanism of the proposed antenna.

state of the designed antenna, two PIN diodes are inserted close to the edge of the slots with diode #4 oriented in the counter-clockwise direction and the diode #5 oriented in the clockwise direction. The proposed antenna has two main polarized states; linear polarization (LP) and circular polarization (CP). The characteristics of this antenna are divided into four cases depending on the bias of the PIN diodes (high-frequency LP, low-frequency LP, RHCP, and LHCP), as shown in Fig. 2.

A. Reconfigurable Polarization

To radiate linearly polarized waves, both PIN diodes on the circular patch (#4 and #5) should be biased in either the "on-state" (*Ant.1*) or the "off-state" (*Ant. 2*) simultaneously, in order to guarantee the physically and electrically symmetric shape of the circular microstrip patch required to excite the TM_{11} mode. When both PIN diodes are in the "on-state," they act as electrically short circuits. Therefore, the conventional circular patch shape is slightly modified with an arc-shaped slot, leading only

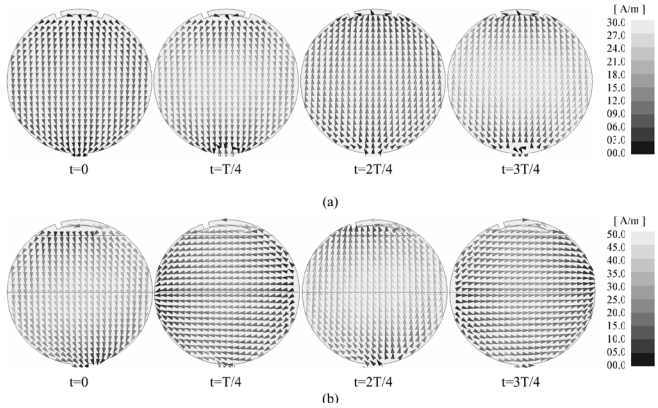

Fig. 3. The electric current distributions on the circular microstrip at their resonant frequencies. (a) "U" shape slot: LP at 2.53 GHz (Ant. 2). (b) "L" shape slot: LHCP at 2.44 GHz (Ant. 3).

to a slight frequency shift without disturbing the radiation pattern. When the two PIN diodes (#4 and #5) on the circular patch are both in the "off-state," they act as electrically open circuits. Hence, the circular patch shape is changed to the circular patch with U-shape slot loading. The difference in the performance between *Ant.1* and *Ant. 2* is the operating frequency. This is due to the different physical antenna sizes (areas) for *Ant.1* is slightly larger than that for *Ant.2*. In other words, the operating frequency of the first configuration is slightly lower than that of the second configuration.

To radiate circularly polarized waves, one of the diodes on the circular patch should be in the "on-state" while the other should be in the "off-state." When diode #4 is in the "off-state" (*open circuit case*) and diode #1 is in the "on-state" (*short circuit case*), this configuration is referred to as *Ant.3*. In this case, the "U" shaped slot in *Ant.2* changes to look like an "L." Since the "L" or inverted-"L" shaped slot perturbs the current along the slot, the excited x-directed (parallel to the horizontal slot orientation) surface current path is lengthened, while the excited y-directed current (orthogonal to the horizontal slot orientation) is slightly affected. Hence the CP can be achieved due to the combination of an almost unchanged TM_{11} mode with the resonance of the slot in the orthogonal direction. Consequently, by choosing the total length of the "L' shaped slot line to be $\lambda_g/4$, the resonant mode in the direction parallel to the long side of the "L" shaped slot can have a slightly lower resonant frequency than the resonant mode in the direction perpendicular to the slot orientation. At the same time, the input reactance of one mode is inductive while that of the other mode is capacitive, which means there are $\pm 90^\circ$ phase difference between the two resonant modes. Therefore, when two near degenerate orthogonal modes of the circular patch antenna are excited with the same amplitude and a 90° phase shift on the circular patch at a given frequency, circular polarization is achieved.

The current distribution at the operating frequency is shown in Fig. 3. As expected, a surface current rotates clockwise for LHCP in *Ant. 3*. In contrast, if PIN diode #4 is in the "on-state" and PIN diode #5 is in the "off-state," the shape of the slot changes to look like an inverted-"L," leading to RHCP in *Ant. 4*. The symmetric shape of these states can easily be observed in these figures due to the symmetry in the antenna's geometry with respect to the feed line.

B. Matching Approach

In [5], it has been observed that the input impedance matching is presented only for circular polarization, because the pattern degrades when the antenna is linearly polarized. In this paper, we use the reconfigurable stub matching approach with three single-stub shunt tuning circuits to address the input impedance matching of linear and circular polarization. When linearly polarized waves (*Ant. 1*) are radiated, PIN diode #1 is in the "on-state" in order to connect between the open-circuit stub (i.e., $S_{O1} : l_1 \times w_1$) to the 50 ohm feed-line, while PIN diodes #2 and #3 are in the "off-state." Similarly, to radiate linearly polarized waves (*Ant. 2*) only PIN diode #2 is in the "on-state" to connect between the open-circuited stub $(S_{O2} : l_2 \times w_2)$ to the 50 ohm feed-line, while PIN diodes #1 and #3 are in the "off-state" with respect to the feed line. To get a good impedance matching for the two circularly polarized states (*Ant. 3* and *4*), the short-circuit stub $(S_{S3} : l_3 \times w_3)$ is connected between the edge of the stub and the ground by using a via hole. There are two main reasons to use the short stub (S_{S3}) instead of an open stub. By using an open stub, the position of the stub will overlap with the neighboring open stubs (S_{O1} or S_{O2}). The other reason is based on the length of the open stub which is longer than that of the short stub by $\lambda_g/4$, which could be large enough (electrically) to radiate. Hence, the stub would no longer be purely reactive [12]. In addition, the elongated stub would increase the overall dimensions of the antenna. Since the input impedance is the same due to the symmetrical geometries with respect to the feed line, it is possible to use the same short stub for both LHCP and RHCP.

C. Application of PIN Diodes

To achieve the reconfigurable polarization capability, switching components must be used. PIN diodes are the most commonly used switching devices for RF and microwave front-end application systems. The RF equivalent circuit of the PIN diode for the ON (forward bias case) and OFF (reverse bias case) states is shown in Fig. 4. The PIN diodes which include self-protect resistors of forward-biased current, RF choke inductors, and dc block capacitors should be isolated from the RF signal. To control the PIN diodes, six dc bias lines are designed with the same size $(l_4 \times w_4)$. The bias circuit must consist of a PIN diode, dc block capacitor, RF choke, and input voltage as shown in Fig. 5. Two dc bias lines are indirectly connected to top part of the circular patch with PIN diodes using "U" shaped slot loading. Three dc bias lines are connected to each matching stub, which supply dc current to PIN diode 1, 2, 3, 4, and 5; the sixth one is used for dc-isolation, which is connected to the 50 Ω feed line. The equivalent RLC circuit models (MA4P274CK-287) that include the parasitic packaging effects can be extracted from the PIN diode data sheet [13]. At the diode on-state, the equivalent circuit is represented by a resistor, $R = 3\Omega$, while the diode off-state, the equivalent circuit is represented by a capacitor, $\mathrm{C} = 0.35$ pF. Three dc block capacitors of $\mathrm{C} = 220$ pF are chosen to isolate the RF components from the dc ones. Since the calculated value of $Zc = -j(1/\omega C) = -j0.3\Omega$ represents a "near short circuit" condition, the RF signal will pass through the capacitor with little loss or reflection. The RF choke inductor isolate the RF signal from flowing into the dc signal, therefore, very thin ($w_4 = 100$ um) quarter-wavelength dc bias lines were used, instead of the RF choke inductors. PIN diodes are used for switching with a forward voltage of $V_F = 0.73V$ and forward bias current of $I_F = 12$ mA, respectively. The photograph of the proposed antenna is shown in Fig. 6.

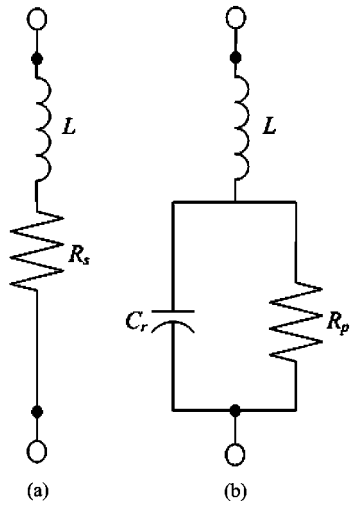

Fig. 4. Equivalent circuit of a packaged PIN diode in its two bias conditions. (a) on-state (forward bias). (b) Off-state (reverse bias). L = 1.4 nH and Rp represents the net dissipative resistance in the reverse biased diode and is less significant.

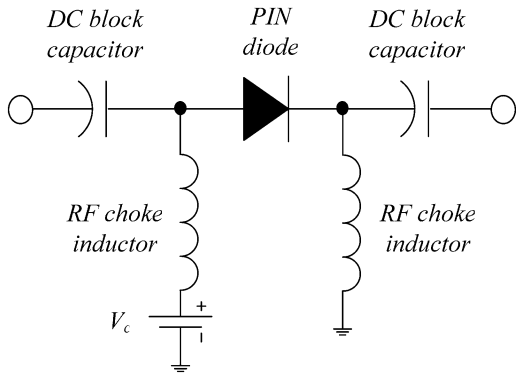

Fig. 5. The configuration in PIN diode biasing circuit.

III. Antenna Performance

The return loss, axial ratio, gain, and radiation patterns of the proposed antenna have been simulated and measured for all the different states of the two PIN diodes (#4 and #5) that control the polarization state as well as for the states of the three PIN diodes (#1, #2 and #3) which connect and disconnect the matching stubs to the feed line. The geometry of the proposed antenna is modified according to the on- and off-states of the PIN diodes and features the resulting capability of polarization diversity. Without loss of generality and for simplicity reasons, an infinite ground plane was used in the simulations, assuming a perfect open-circuit (gap) for the PIN diodes in the off-state. When the diodes are in the on-state, they were modeled as through lines by using metal tape (1.94×1.60 mm^2).

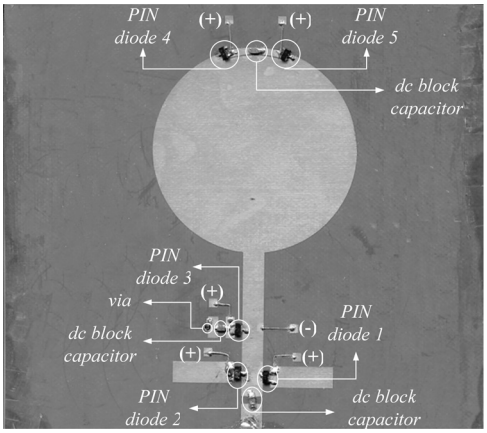

Fig. 6. Photograph of the single-feed circular microstrip antenna for reconfigurable polarization capability.

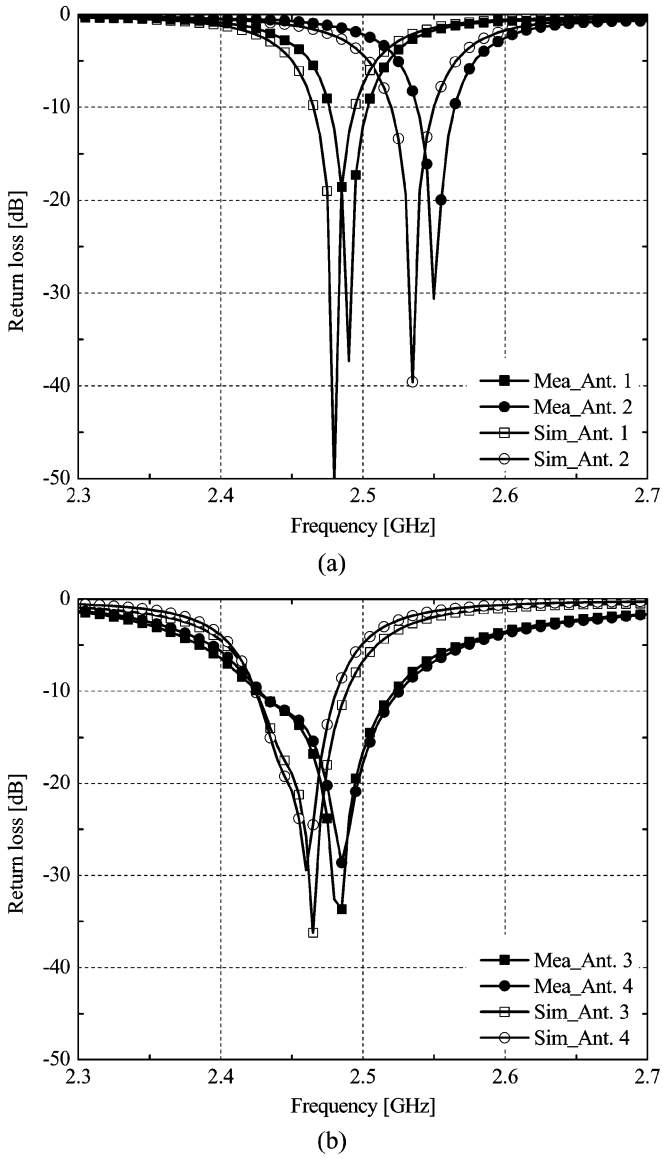

Fig. 7. Simulated and measured return loss of the proposed antenna for (a) LP and (b) CP sense: $\mathrm{r1} = 23\ \mathrm{mm}, \mathrm{r2} = 21\ \mathrm{mm}, \alpha = 40°, \mathrm{s1} = 14.45\ \mathrm{mm}, \mathrm{l1} = 4.85\ \mathrm{mm}, \mathrm{w1} = 7.73\ \mathrm{mm}, \mathrm{s2} = 24.45\ \mathrm{mm}, \mathrm{l2} = 4.85\ \mathrm{mm}, \mathrm{w2} = 20.32\ \mathrm{mm}, \mathrm{s3} = 25.36\ \mathrm{mm}, \mathrm{l3} = 4.85\ \mathrm{mm}, \mathrm{w3} = 15.79\ \mathrm{mm}, \mathrm{w4} = 1.94\ \mathrm{mm}, \mathrm{l4} = 1.60\ \mathrm{mm}$ and $\mathrm{g} = 0.2$ mm.

The simulations of the proposed antenna were carried out using IE3D, a commercial electromagnetic simulator based on the integral equation method and the method of moments. It is observed that good impedance matching can be achieved for all polarization (LP and CP) states, as shown in Fig. 7. The difference in the results between the simulated and measured data is due to the use of an infinite ground in the simulation.

Details of the design parameters and the obtained results for the four different antenna prototypes are summarized in Table I. The bandwidth for the CP (2.60 % for *Ant. 3*) is much larger than that of the LP (1.17 % for *Ant. 1*) because two resonant modes radiate simultaneously for the circular polarized case, and only one resonant mode (TM_{11}) radiates for the linear polarized case which is similar to the mode of the conventional circular microstrip patch. The simulated and measured axial ratios of the proposed antenna for CP (*Ant. 3* and *Ant. 4*) are shown in Fig. 8 where very good agreement is observed. The minimal difference of the minimum AR point between Ant. 3 and Ant. 4 (less than 5 MHz) in simulation can be attributed to the non-symmetry of the matching stubs. Fig. 9 shows the simulated gain of the proposed antenna for LP and CP states, which is near 6 dBi across the operational bandwidth. Fig. 10 shows the simulated and measured radiation patterns at 2.477 GHz and 2.552 GHz for the LP states (*Ant. 1* and *Ant. 2*). The peak gains are observed to be 5.85 dBi and 5.94 dBi for Ant. 1 and Ant. 2, respectively. The cross polarization level is below -20 dB at each given frequency in both *Ant. 1* and *Ant. 2*, which have good LP antenna performance. There is a discrepancy between the simulated and measured cross-polarization patterns. The slight frequency shift between the measurements and the experimental results can be attributed to SMA connector interference and other chamber uncertainties. Fig. 11 shows the simulated and measured radiation patterns at 2.445 and 2.450 GHz for the CP states (*Ant. 3* and *Ant. 4*). Good agreement is observed in the main beam of the co-polarization (i.e., the left-hand circular polarization, LHCP). The level of cross-polarization (i.e., the right-hand circular polarization, RHCP) is lower than -20 dB over the main beam direction in *Ant. 3*. Similar radiation patterns have been observed in *Ant. 4* due to their symmetric topologies with respect to the feed line. It is also observed that the difference between the co-polarized radiation (i.e., the right-hand circular polarization, RHCP) and cross-polarized radiation (i.e., the left-hand circular polarization, LHCP) is more than 20 dB over the broadside direction for *Ant. 4*. The simulated and measured frequencies for the radiation patterns in the circularly polarized states were selected at the minimum axial ratio in the operating bandwidth (AR $\leq$ 3 dB). Measured radiation patterns (*Ant. 1, 2, 3,* and *4*) show that broadside radiation patterns with good LP and CP characteristics are obtained at the respective resonant frequency.

IV. Parametric Study and Design Procedure

A. Design Frequency

The resonant frequency of a circular microstrip patch antenna for the TM_{nm} mode can be evaluated from following equation [1].

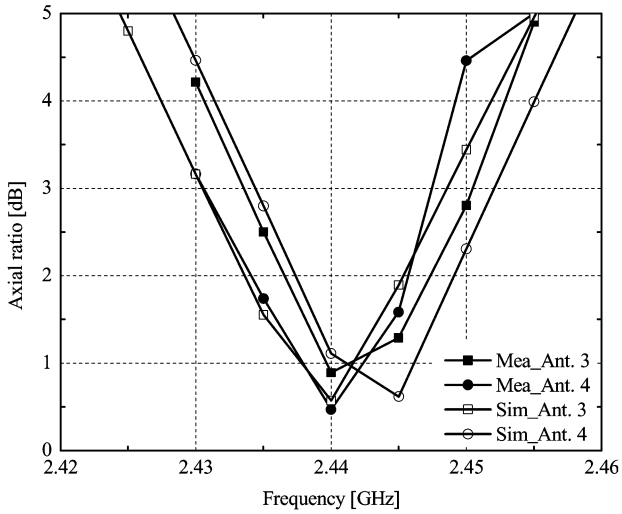

Fig. 8. The simulated and measured axial ratio of the proposed antenna in *Ant. 3* and *Ant. 4*.

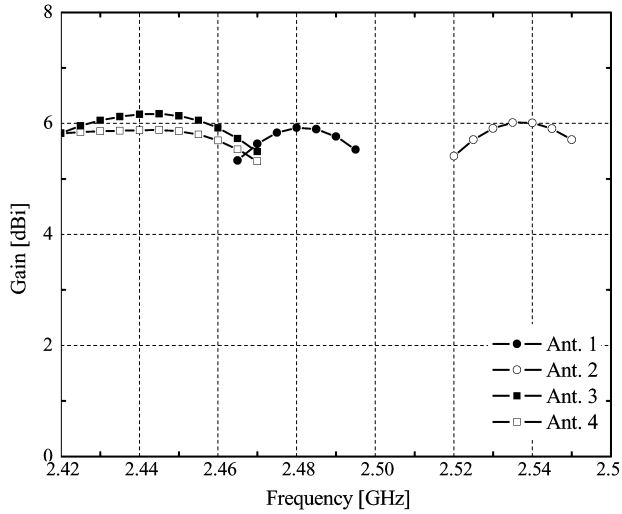

Fig. 9. The gain of the proposed antenna in *Ant. 1, 2, 3,* and *4.*

Thus

$$f_{nm} = \frac{\chi_{nm} C}{2\pi r_e \sqrt{\varepsilon_r}} \tag{3}$$

$$r_e = r\left\{1 + \frac{2h}{\pi r \varepsilon_r}\left(\ln\frac{\pi r}{2h} + 1.7726\right)\right\}^{1/2} \tag{4}$$

where r_e is an effective radius, h is a thickness of substrate, χ_{nm} represents the zeroes of the derivative Bessel function $J_m(x)$, and these zeroes determine the order of the resonant frequencies. Since the first value of χ_{nm} is $\chi_{11} = 1.8412$, for the geometrical parameters of the prototyping antenna (radius of $\mathrm{r} = 23$ mm and substrate thickness of $\mathrm{h} = 1.575$ mm) the calculated resonant frequency is 2.46 GHz which can be applied in WLAN band. Fig. 12 shows the concept of the design frequency in the parametric study regarding different shape of the circular microstrip patch. Step 1 is the conventional circular patch, step 2 (mentioned as Ant. 1) is the circular patch with "arc" shape slot, step 3 (mentioned as Ant. 2) is the circular patch with "U" shape slot, and step 4 is the circular patch with circular segment notch, respectively. The radius (i.e., $\mathrm{r} = 23$ mm) which is determined from center of the circular patch to the outer boundary is fixed at all steps. Fig. 13 shows the simulated return loss plots for the four different types of the circular microstrip shape. The

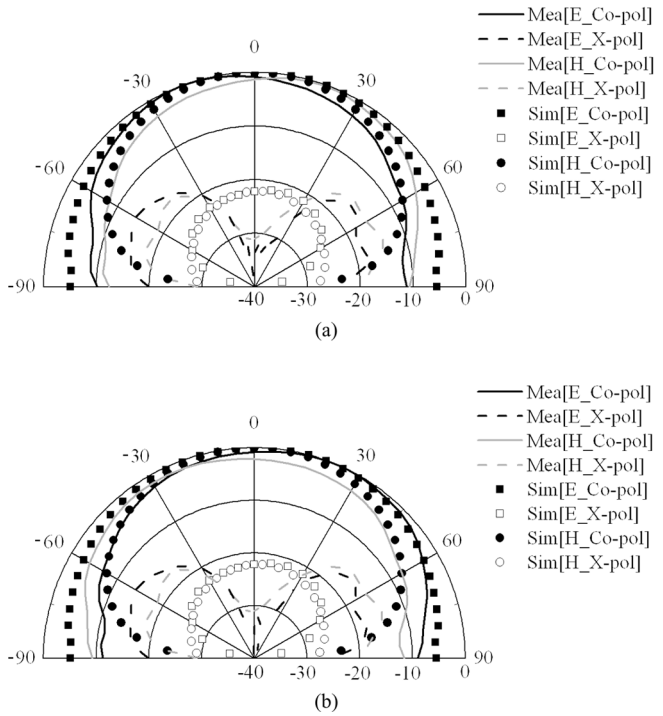

Fig. 10. Simulated and measured radiation patterns of the proposed antenna for linear polarization sense (a) *Ant. 1* and (b) *Ant. 2*.

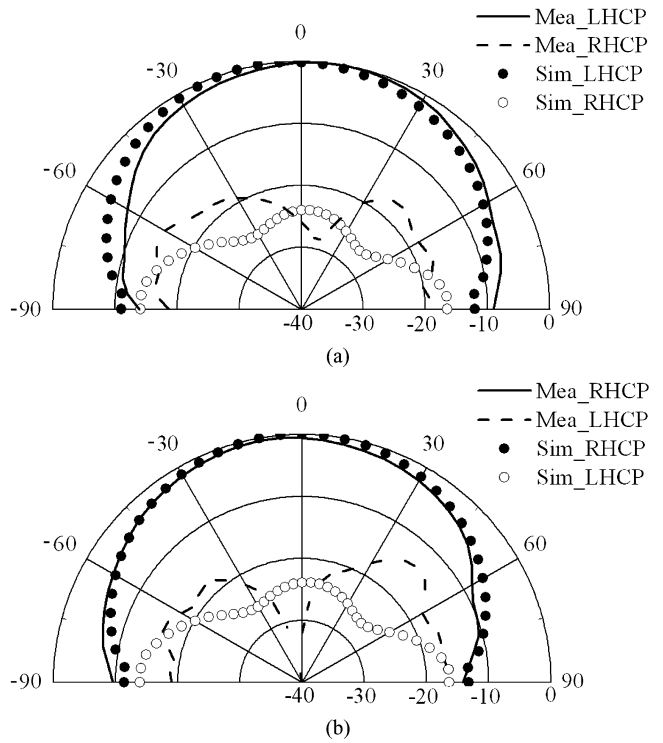

Fig. 11. Simulated and measured radiation patterns of the proposed antenna for circular polarization sense (a) *Ant. 3* and (b) *Ant. 4*.

TABLE I
DETAILS OF OBTAINED SIMULATED AND EXPERIMENTAL RESULTS FOUR DIFFERENT ANTENNA PROTOTYPES

	Diode 1	Diode 2	Diode 3	Diode 4	Diode 5	Polarization	S11 [dB]		-10 dB BW [%]		3 dB Axial ratio BW [%]	Gain [dBi]
							Sim.	Mea.	Sim.	Mea.		
Ant. 1	on	off	off	on	on	LP	-50.14	-39.57	1.17	1. 19	N/A	5.85
Ant. 2	off	on	off	off	off	LP	-39.57	-30.62	1.18	1.17	N/A	5.85
Ant. 3	off	off	on	off	on	LHCP	-36.21	-32.58	3.60	4.04	0.74	5.95
Ant. 4	off	off	on	on	off	RHCP	-29.43	-28.64	3.63	4.02	0.72	5.94

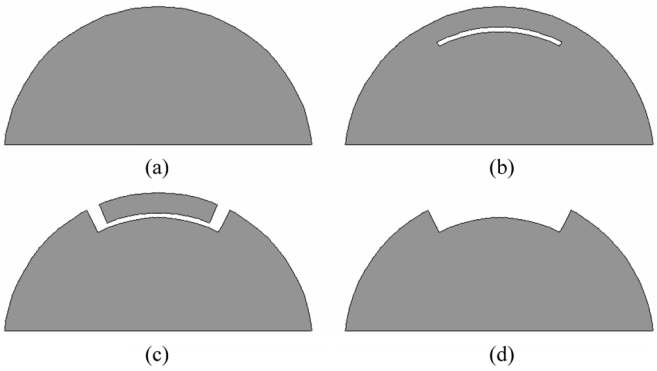

Fig. 12. The concept of the design frequency in the parametric study.

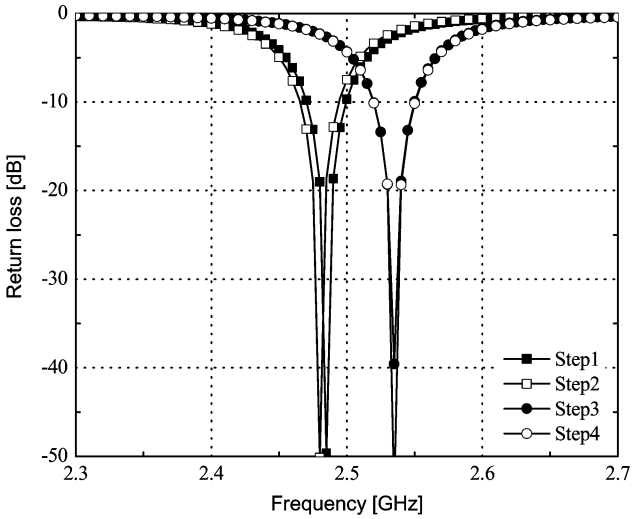

Fig. 13. The simulated return loss plots for the four different types of the circular microstrip shape.

operating frequency of the step 2 is much slightly lower than one of the step 1 because of the "arc" shape slot which slightly increases the current patch. As mentioned above Section II-A, the physical dimension of the circular patch at step 3 is smaller than one of the circular patch at step 2. Hence, the operating frequency of the step 3 is higher than one of the step 2, which leads to the reconfigurable frequency antenna in LP. The operating frequency of step 4 is almost same to the one of step 3 due to the same size of the radiating elements. In other words, the shape of the step 3 is same to the shape of the step 4 adding ring segment which is a non-radiating element.

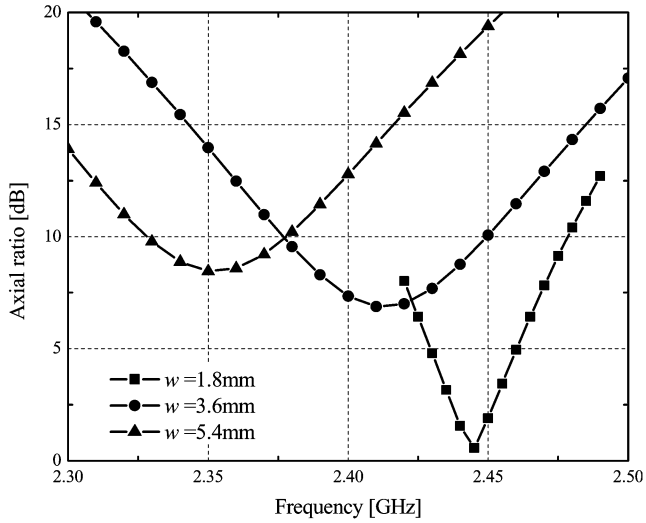

Fig. 14. Simulated the axial ratio for different length of inset.

B. Adjusting Inset Length to Obtain the Circular Polarization

Fig. 14 shows the axial ratio for different lengths of the inset (w). (In this study, only the length of the inset is varied while the total "L" shaped slot length is fixed). When the length of the inset is a minimum, a good axial ratio can be achieved, which means that the excited x-directed surface current path is mostly affected while the excited y-directed surface current path is slightly affected. Hence, the CP can be generated with same amplitude and a 90 degrees phase difference. When the ratio of the total length of slot to the length of the inset is maximum, a good axial ratio can be accomplished as shown in Fig. 14. Since the width of the PIN diode implemented on the circular patch is 1.8 mm, we considered the length of the inset to be greater than 1.8 mm.

C. Obtain a Satisfactory Input Impedance Bandwidth of Circular Polarization

The circular polarization performance of the proposed antenna is mainly determined by the central angle of the "L" shaped slot. Fig. 15 shows the effect of increasing the central angle (α°) from 30 deg. to 50 deg. (step is 10 deg.) on the input impedance locus similar to those for Ant. 1 and 2. It can be observed from Fig. 15(a) and (b) that this effect is very similar for the two linear polarization configurations of Ant.1 ("arc" shaped slot) and Ant.2 ("U" shaped slot) due to the fact that the feed line is place at the center (dichotome) of r.

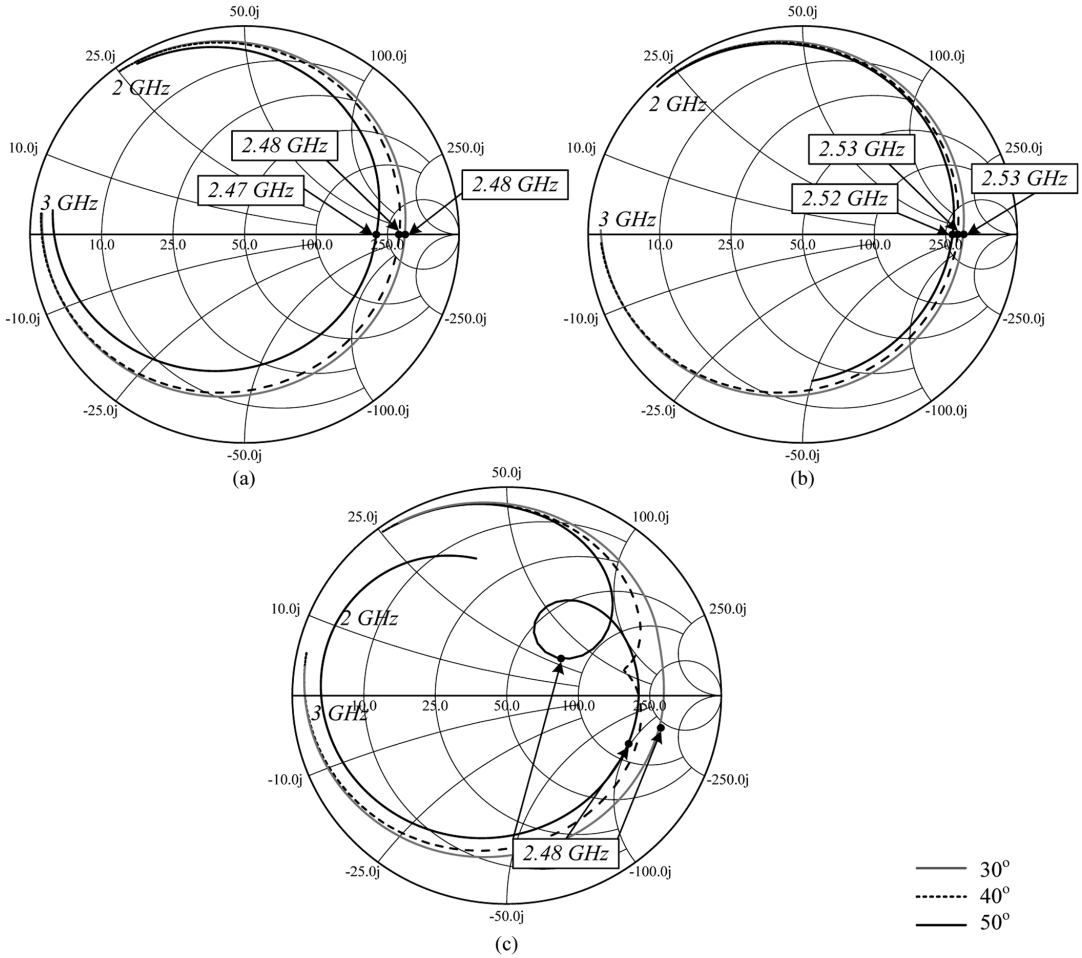

Fig. 15. Simulated input impedance results for various angle of the slot. (a) "Arc" shape for Ant. 1. (b) "U" shape for Ant. 2. (c) "L" shape for Ant. 3.

Therefore, these two cases for Ant. 1 and 2 are observed for linear polarization. Fig. 15(c) illustrates the impedance locus for circular polarization. A good input impedance performance is observed if the central angle is 40° for circular polarization due to the fact that the effective total "L" shaped slot length is approximately a quarter wavelength at given frequency. Hence, the impedance curve at 40° has the sharpness tip of the kink in the Smith chart enabling the best circular polarization performance. It has to be noted that the shape of this impedance curve is a result of having two orthogonal modes with slightly different resonant frequencies.

D. Adjusting β° to Obtain a Good Axial Ratio

After adjusting the central angle of the slot, the optimum axial ratio that best characterizes circular polarization is investigated by fine tuning the shifting angle (β°) which is defined as the angle between the midpoint on the "arc" shaped slot and the Y-axis.

In the simulation, we adjust β with the fixed length of the "arc" shaped slot to observe how beta could control the tip of kink in input impedance locus which is directly related to the axial ratio for circular polarization. Fig. 16 describes the variation of the input impedance for Ant. 3 (CP) at different values of angle (β°). It is observed that a tip of the kink is sharper when

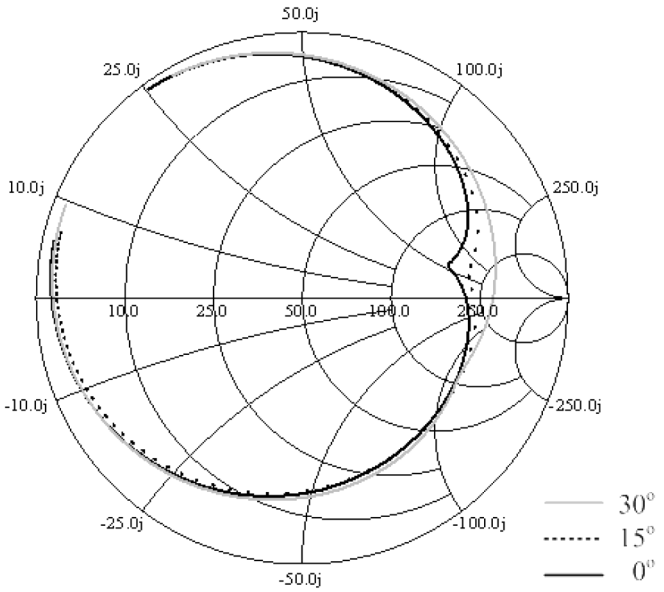

Fig. 16. Simulated the input impedance locus for varying shifting angle (β°) of the "L" shape slot.

the shifting angle is 0°, because the excited x-directed (orthogonal to the slot orientation) and the excited y-directed (parallel

to the slot orientation) currents can constitute the optimum combination of the two-orthogonal-near-degenerate modes for this topology.

V. Conclusion

The design of a novel single feed microstrip antenna with reconfigurable polarization capabilities has been presented in this paper. Unlike the conventional switchable polarizations studied in past literature, the proposed antenna can be switched by controlling the PIN diodes for low frequency and high frequency modes in linear polarization, as well as for LHCP and RHCP in circular polarization. A good impedance matching performance for all polarization senses is observed using open and short stubs. All of the simulated and measured results agree very well confirming the validity of our theory and the used models. By using the suitable switching devices (i.e., MEMS switch), the proposed antenna can be used in higher frequency commercial and military applications. It has to be noted that the proposed antenna design is desirable for many wireless communication applications such as wireless local area network (WLAN), satellite links, global positioning system (GPS) and space robots.

Acknowledgment

The authors would like to acknowledge the assistance from Dr. R. Li and G. DeJean.

References

[1] F. Yang and Y. Rahmat-Samii, "A reconfigurable patch antenna using switchable slots for circular polarization diversity," *IEEE Microw. Wireless Comp. Lett.*, vol. 12, no. 3, pp. 96–98, Mar. 2002.

[2] M.-H. Ho, M.-T. Wu, C.-I. G. Hsu, and J.-Y. Sze, "An RHCP/LHCP switchable slotline-fed slot-ring antenna," *Microw. Opt. Technol. Lett.*, vol. 46, no. 1, pp. 30–33, Jul. 2005.

[3] H. Chuang, L. Kuo, C. Lin, and W. Chen, "A 2.4 GHz polarization-diversity planar printed antenna for WLAN and wireless communication systems," in *Proc. IEEE Antennas and Propag. Society Int. Symp.*, Jun. 2002, vol. 4, pp. 76–79.

[4] F. Yang and Y. Rahmat-Samii, "Patch antenna with switchable slots (PASS) in wireless communication: Concepts, designs, and applications," *IEEE Trans. Antennas Propag.*, vol. 47, no. 2, Apr. 2005.

[5] M. K. Fries, M. Gräni, and R. Vahldieck, "A reconfigurable slot antenna with switchable polarization," *IEEE Microw. Wireless Compon. Lett.*, vol. 13, no. 11, pp. 490–492, Nov. 2003.

[6] N. Jin, F. Yang, and Y. Rahmat-Samii, "A novel patch antenna with switchable slot (PASS): Dual-frequency operation with reversed circular polarizations," *IEEE Trans. Antennas Propag.*, vol. 54, no. 3, pp. 1031–1034, Mar. 2006.

[7] M. Boti, L. Dussopt, and J.-M. Laheurte, "Circularly polarized antenna with switchable polarization sense," *Electron. Lett.*, vol. 36, no. 18, pp. 1518–1519, Aug. 2000.

[8] Y. J. Sung, T. U. Jang, and Y.-S. Kim, "A reconfigurable microstrip antenna for switchable polarization," *IEEE Microw. Wireless Compon. Lett.*, vol. 14, no. 11, pp. 534–536, Nov. 2004.

[9] S. Nikolaou, R. Bairavasubramanian, C. Lugo, I. Carrasquillo, D. C. Thompson, G. E. Ponchak, J. Papapolymerou, and M. M. Tentzeris, "Pattern and frequency reconfigurable annular slot antenna using PIN diodes," *IEEE Trans. Antennas Propag.*, vol. 54, no. 2, pp. 439–449, Feb. 2006.

[10] K. Chang, I. Bahl, and V. Nair, *RF and Mircrowave Circuit and Component Design for Wireless Systems*. New York: Wiley-Interscience, 2002.

[11] *Zeland's IE3D* 2004, Release 10.

[12] D. M. Pozar, *Microwave Engineering*, 2nd ed. New York: Wiley, 1998.

[13] *Data Sheet of MA4P274CK PIN Diodes*, , MA-Com, Application Note.

Boyon Kim (S'05) received the B.S. and M.S. degrees from Korea University, Seoul, Korea, in 2003 and 2007, respectively.

Since 2007, he has been an SoC Product and Test Engineer with System LSI Division, Semiconductor Business, Samsung Electronics Co., Ltd., Giheung, Korea, where he has been involved in RF Mobile PE and Test team. His research interests include Ultra-wideband (UWB) systems, orthogonal frequency division multiplexing (OFDM), and developing the test methods for mixed signal systems.

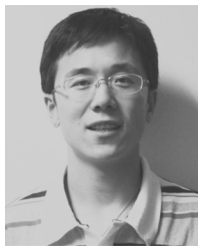

Bo Pan (S'03) received the B.S. and M.S. degrees from Tsinghua University, Beijing, China, in 2000 and 2003, respectively. He is currently working toward the Ph.D. degree in electrical and computer engineering at the Georgia Institute of Technology, Atlanta.

His research involves the design, processing and characterization of novel micromachined passive components for RF/Microwave/Millimeter-wave front-ends. He is also researching antenna designs for GPS/IMT-2000/WLAN/WiMAX applications.

Symeon Nikolaou received the Diploma in Electrical and Computer Engineering from the National Technical University of Athens (NTUA), Athens, Greece, in 2003 and the M.S.E.C.E. and Ph.D. degrees from Georgia Institute of Technology, Atlanta, in 2005 and 2007, respectively.

His current research interests include the design and development of compact UWB and reconfigurable antennas, the development of RFIDs, and RF packaging and design.

Young-Sik Kim (S'82–M'86) received the B.S. degree in electronics engineering from Korea University, Seoul, in 1973, and the M.S. and Ph.D. degrees in electrical engineering from the University of Massachusetts at Amherst, in 1986 and 1988, respectively.

From 1988 to 1989, he was a Postdoctoral Research Fellow at the University of Massachusetts at Amherst. From 1989 to 1993, he was with the Mobile Communications Division, Korea Electronics and Telecommunications Research Institute, Daejeon. Since 1993, he has been with the Department of Radio Sciences and Engineering, Korea University, where he is currently a Professor. His main field of interest is millimeter-wave antennas and front-end systems and mobile telecommunication systems.

John Papapolymerou (S'90–M'99–SM'04) received the B.S.E.E. degree from the National Technical University of Athens, Athens, Greece, in 1993, and the M.S.E.E. and Ph.D. degrees from the University of Michigan, Ann Arbor, in 1994 and 1999, respectively.

From 1999 to 2001, he was an Assistant Professor in the Department of Electrical and Computer Engineering, University of Arizona, Tucson, and during summers 2000 and 2003 he was a Visiting Professor at the University of Limoges, France. From 2001 to 2005, he was an Assistant Professor at the School of Electrical and Computer Engineering, Georgia Institute of Technology (Georgia Tech), Atlanta, where he is currently an Associate Professor. His research interests include the implementation of micromachining techniques and MEMS devices in microwave, millimeter-wave and THz circuits and the development of both passive and active

planar circuits on semiconductor (Si/SiGe, GaAs) and organic substrates (LCP, LTCC) for system-on-a-chip (SOC)/ system-on-a-package (SOP) RF front ends. He has authored or coauthored over 140 publications in peer reviewed journals and conferences.

Dr. Papapolymerou received the 2004 Army Research Office (ARO) Young Investigator Award, the 2002 National Science Foundation (NSF) CAREER award, the Best Paper Award at the 3rd IEEE International Conference Microwave and Millimeter-Wave Technology (ICMMT2002), Beijing, China, and the 1997 Outstanding Graduate Student Instructional Assistant Award presented by the American Society for Engineering Education (ASEE), University of Michigan Chapter. His student also received the Best Student Paper Award at the 2004 IEEE Topical Meeting on Silicon Monolithic Integrated Circuits in RF Systems, Atlanta, GA. He currently serves as the Vice-Chair for Commission D of the U.S. National Committee of the URSI and as an Associate Editor for the IEEE MICROWAVE AND WIRELESS COMPONENT LETTERS and the IEEE TRANSACTIONS ON ANTENNAS AND PROPAGATION. During 2004 he was the Chair of the IEEE MTT/AP Atlanta Chapter.

Manos M. Tentzeris (S'89–M'98–SM'03) received the Diploma Degree in Electrical and Computer Engineering (*magna cum laude*) from the National Technical University of Athens, Athens, Greece and the M.S. and Ph.D. degrees in electrical engineering and computer science from the University of Michigan, Ann Arbor.

He is currently an Associate Professor with School of School of Electrical and Computer Engineering, Georgia Institute of Technology (Georgia Tech), Atlanta. He has published more than 260 papers in refereed journals and conference proceedings, two books, and ten book chapters. He has helped develop academic programs in highly integrated/ multilayer packaging for RF and wireless applications using ceramic and organic flexible materials, paper-based RFID's and sensors, microwave MEM's, SOP-integrated (UWB, multiband, conformal) antennas and adaptive numerical electromagnetics (FDTD, multiresolution algorithms) and heads the ATHENA Research Group, Georgia Tech, (20 researchers). He is the Georgia Electronic Design Center Associate Director for RFID/sensors research, and he has been the Georgia Tech NSF-Packaging Research Center Associate Director for RF Research and the RF Alliance Leader from 2003–2006. He was a Visiting Professor with the Technical University of Munich, Germany for summer 2002, where he introduced a course in the area of high-frequency packaging. He has given more than 50 invited talks in the same area to various universities and companies in Europe, Asia, and America.

Dr. Tentzeris was the recipient/co-recipient of the 2007 IEEE APS Symposium Best Student Paper Award, the 2007 IEEE IMS Third Best Student Paper Award, the 2007 ISAP 2007 Poster Presentation Award, the 2006 IEEE MTT Outstanding Young Engineer Award, the 2006 Asian-Pacific Microwave Conference Award, the 2004 IEEE TRANSACTIONS ON ADVANCED PACKAGING Commendable Paper Award, the 2003 NASA Godfrey "Art" Anzic Collaborative Distinguished Publication Award, the 2003 IBC International Educator of the Year Award, the 2003 IEEE CPMT Outstanding Young Engineer Award, the 2002 International Conference Microwave and Millimeter-Wave Technology Best Paper Award (Beijing, China), the 2002 Georgia Tech-ECE Outstanding Junior Faculty Award, the 2001 ACES Conference Best Paper Award and the 2000 NSF CAREER Award, and the 1997 Best Paper Award of the International Hybrid Microelectronics and Packaging Society. He was also the 1999 Technical Program Co-Chair of the 54th ARFTG Conference, Atlanta, and the Chair of the 2005 IEEE CEM-TD Workshop. He is the Vice-Chair of the RF Technical Committee (TC16) of the IEEE CPMT Society. He has organized various sessions and workshops on RF/Wireless Packaging and Integration, RFID's, Numerical Techniques/Wavelets, in IEEE ECTC, IMS, VTC and APS Symposia in all of which he is a member of the Technical Program Committee in the area of "Components and RF." He will be the TPC Chair for IEEE IMS 2008 Symposium. He is an Associate Editor of the IEEE TRANSACTIONS ON ADVANCED PACKAGING. He is a member of URSI Commission D, the MTT-15 Committee, an Associate Member of EuMA, a Fellow of the Electromagnetic Academy, and a member of the Technical Chamber of Greece.